Int. J. Electrochem. Sci., 17 **(2022)** Article Number: 221045, doi: 10.20964/2022.10.29

International Journal of
ELECTROCHEMICAL
SCIENCE
www.electrochemsci.org

Application of WO_3 and Zn-doped WO_3 prepared by microwave irradiation for photocatalytic degradation of Rhodamine B in water and wastewater

Xinmin Ding[1], *Wanli Liu*[1,2,*], *Yi Feng*[1,2], *Jian Liu*[1,2], *Xuebing Zeng*[1], *Ran Zhou*[1,2], *Xiaoya Zhang*[1], *Rui Wang*[1], *Qi Guo*[1]

[1] West China Tianfu Hospital of Sichuan University, Chengdu, China
[2] West China Hospital of Sichuan University, Chengdu, China
[*]E-mail: HXYY_ding@163.com

Received: 17 July 2022 / *Accepted:* 17 August 2022 / *Published:* 10 September 2022

This research focused on the structural, optical, and electrochemical characterization of WO_3 and Zn-doped WO_3, as well as their application as photocatalysts for the degradation of Rhodamine B (RhB), a growing organic contaminant from water and wastewater, when exposed to visible light. According to structural analyses, microwave irradiation successfully generated nanorod-shaped WO_3 and Zn-doped WO_3 structures. The optical band gap values of WO_3 and Zn-doped WO_3 structures were determined to be 3.12 and 2.83 eV, respectively, resulting in quick charge transfer and leading to an increase in the photocatalytic activity of the Zn-doped WO_3 structure under visible light irradiation. According to electrochemical experiments, the lifespan of photo-generated electrons in Zn-doped WO_3 was longer than that of WO_3, indicating that Zn-doped WO_3 had the highest separation efficiency and the fastest diffusion rate. The entire degradation efficiency of 150 mL of 10 mg/L RhB solution was reached after 30 and 15 minutes of visible light irradiation in current WO_3 and Zn-doped WO_3, respectively, according to the photodegradation assays. The photocatalytic degradation capability of Zn-doped WO_3 was tested for the treatment of 150 mL of 5 mg/L RhB solution prepared from real textile effluent, and the results confirmed that Zn-doped WO_3 has a high photocatalytic activity when exposed to visible light for the treatment of RhB from real textile effluent.

Keywords: Photocatalyst; WO_3; Zn-doped WO_3; Rhodamine B; Organic pollutants; Textile effluent

1. INTRODUCTION

Rhodamine B (RhB) is an organic chloride salt with the counter ion N-[9-(2-carboxyphenyl)-6-(diethylamino)-3H-xanthen-3-ylidene]-N-ethylethanaminium [1, 2]. It's a fluorochrome that's made up of amphoteric dyes [3, 4]. It is frequently utilized in biotechnology applications such as fluorescence microscopy, flow cytometry, fluorescence correlation spectroscopy, and ELISA as a fluorochrome,

fluorescent probe, and histology dye [5-7]. RhB is a xanthene dye that is widely used in the textile, paper, paint, food, and leather industries for printing and dyeing [8-10]. Food safety officials have been aware of cases of commercially driven adulteration, in which it has been unlawfully used to lend a red hue to chili powder [11, 12]. RhB is a common contaminant found in industrial wastewater [13-15].

RhB is a poisonous dye because of its carcinogenic and neurotoxic properties, as well as its capacity to cause a variety of disorders in people [16, 17]. When it mixes with food and water, it enters the body and causes oxidative stress in cells and tissues [18], and may cause gastrointestinal irritation with nausea, vomiting and diarrhea [19, 20]. As a result of these substantial environmental and biological issues, removing RhB from wastewater is a significant challenge. Liquid membrane [21], ozonation [22], adsorption [23, 24], Fenton pre-oxidation [25], electro-biodegradation process [26] and photocatalysis [27-32] are the conventional methods for treatment of RhB. Many of these treatment procedures are costly and ineffective, because they cause chemical bonds to break or breakdown, resulting in a substantial amount of secondary contamination [33-35]. Photocatalysis is a cost-effective and affordable oxidation technology for treating dye-contaminated wastewater in the presence of photocatalysts, and it is an efficient and sustainable oxidation technique.

Therefore, the focus of this research was on the preparation of WO_3 and Zn-doped WO_3 using the microwave irradiation method, as well as structural, optical, and electrochemical characterizations, and application as photocatalysts for the degradation of RhB, an emerging organic pollutant from water and wastewater, when exposed to visible light.

2. EXPERIMENT

2.1. Preparation of WO_3 and Zn-doped WO_3

The microwave irradiation method was used for the synthesis of Zn-doped WO_3 as follows [36]: 0.1 g of tungstic acid (≥99%, Sigma-Aldrich) and 0.05 g of zinc nitrate hexahydrate (≥99.0%, Sigma-Aldrich) were added to 100 mL of 0.5M sodium hydroxide (≥97.0%, Sigma-Aldrich) solution. To obtain precipitates, the liquid was magnetically stirred for 25 minutes. After that, the precipitate was washed three times with deionized water to remove any unreacted chemical species from the reaction mixture. The precipitates were then dried for 10 hours in a vacuum oven. Microwave (2.45 GHz) radiation with a most constructive power of 160 W was applied to the dried precipitates for 15 minutes in an ambient atmosphere to produce a light greenish yellow powder as Zn-doped WO_3. The same technique was used for pure WO_3 without zinc nitrate hexahydrate.

2.2. Photodegradation tests

On visible light irradiation, photodegradation studies of WO_3 and Zn-doped WO_3 towards the degradation of RhB dye were carried out in a Pyrex flask type reactor. A 400 W Xe lamp (Guangzhou Deao Light Source Technology Co., Ltd., China) was mounted on top of the reactor and emitted visible light. Under steady stirring, 0.2 g of synthesized photocatalysts were added to 150 mL of RhB

dye solutions for photodegradation. The suspension was magnetically agitated in the dark for 40 minutes prior to visible light irradiation to achieve the desorbance-absorbance balance. The stable suspension was then exposed to visible light for a photocatalytic reaction while being constantly stirred. The photodegraded RhB sample was removed at regular intervals and collected, then centrifuged for 10 minutes at 1500 rpm to remove photocatalyst particles. Finally, the absorption spectrum of photodegraded RhB using a UV–visible spectrophotometer (2550-Shimadzu, Japan) at λ=554 nm was employed to calculate the degradation efficiency (ξ) by the following equation [30]:

$$\xi\ (\%) = \frac{C_0 - C_t}{C_0} \times 100 \qquad (1)$$

Where C_0 is initial concentration of the RhB and C_t is concentration of the RhB after visible light irradiation.

2.3. Characterizations

The morphology and structure of photocatalysts were studied using a scanning electron microscope (SEM; JEOL JSM-6390, Japan) and X-ray difraction (XRD; Bruker D8 Advanced difractometer, AXS, Karlsruhe, Germany). A spectrometer was used to measure UV–vis absorption spectra (2550-Shimadzu, Japan). Electrochemical impedance spectroscopy (EIS) measurements were performed on a traditional three-electrode system containing a photocatalyst modified Indium tin oxide (ITO), Pt foil, and Ag/AgCl electrode as a working, counter, and reference electrode, respectively, on an electrochemistry workstation (CHI 660E, Chenhua Technology Co., Ltd., Shanghai, China). EIS experiments were carried out in solution containing solution containing a frequency range of 10^{-2}–10^{4} Hz with 10 mV amplitude.

3. RESULTS AND DISCUSSION

3.1. Study of morphology and structure of photocatalysts

The SEM pictures of WO_3 and Zn-doped WO_3 structures are shown in Figure 1. Figure 1a shows homogeneous nanorods with cuboid-like cross sections with an average width of 160nm and a length of 700nm on the surface of the WO_3 nanostructure. Figure 1b shows a SEM picture of a Zn-doped WO_3 structure with irregular nanorod shapes with average diameters of 150nm and average lengths of 650nm.

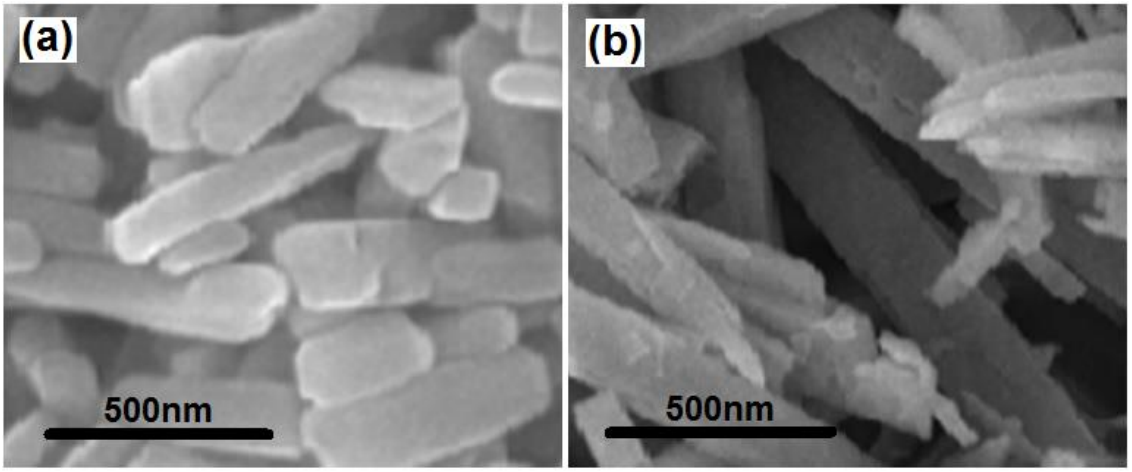

Figure 1. SEM images of (a) WO_3 and (b) Zn-doped WO_3.

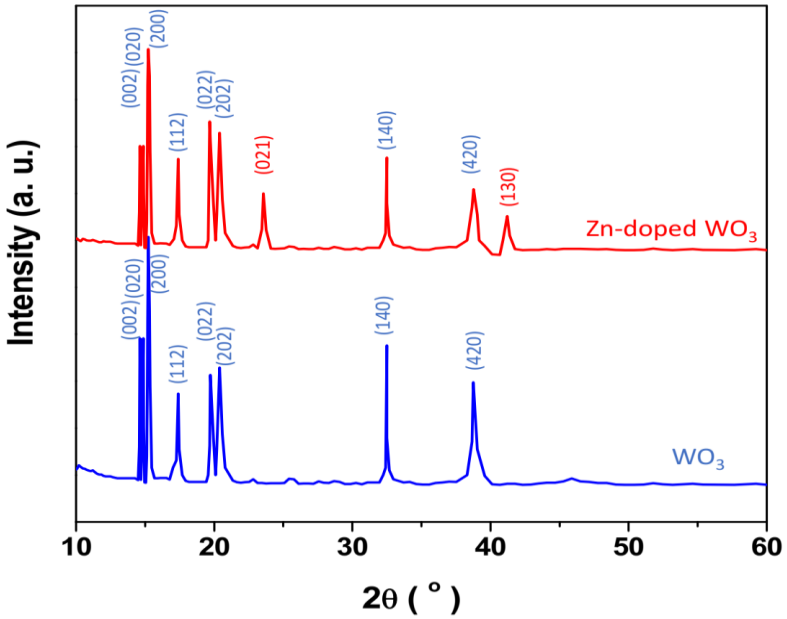

Figure 2. XRD patterns of WO_3 and Zn-doped WO_3.

Figure 2 shows the XRD patterns of WO_3 and Zn-doped WO_3. XRD patterns of WO_3 and Zn-doped WO_3 display characteristic peaks at 2θ=14.63°, 14.85°, 15.25°, 17.39°, 19.71°, 20.45°, 32.47°, and 38.75°, which correspond to the (002), (020), (200), (112), (022), (202), (140), and (420) planes, respectively (JCPDS card no. 43-1035) [37-39]. The XRD pattern of Zn-doped WO_3 shows two extra faint diffraction peaks in the (021) and (130) planes, respectively, which correspond to the monoclinic structure of $ZnWO_4$ (JCPDS card no. 15-0774) [40-42]. The XRD patterns of both samples show that the microwave irradiation approach successfully produced WO_3 and Zn-doped WO_3.

3.2. Optical properties of photocatalysts

Figure 3a shows the UV–vis absorption spectra of WO_3 and Zn-doped WO_3. Both nanostructures absorb light in the UV and visible spectrums. Pure WO_3 has a 470 nm absorption start in its UV–vis absorption spectra [43-45]. The doped sample shows a slight redshift in absorption onset to 500 nm. It is associated with the fact that Zn is the conductive metal and addition in the WO_3 structure which increases in absorbance due to the presence of metal ion (Zn^{2+}) [46], due to generation of the intermediate energy level and electronic transitions between localized energy levels between the blocked conduction band and unblocked valance band which improves the light absorption ability in both UV and visible regions [47-49]. Photo-generated electrons can be trapped by defects, resulting in rapid charge transfer and separation [50]. Furthermore, Zn doping causes the absorbance onset to tail into the visible range, indicating the development of oxygen vacancies during nucleation growth in microwave conditions and the production of the Zn–O–W link, which is compatible with the XRD results [51-53]. It can increase of carriers with high mobility and thus improving the separation and injection efficiency of carriers [54, 55]. The band gap energy (Eg) value for samples can be estimated using the following equation [56, 57]:

$$(\alpha h\nu)^2 = A(h\nu - Eg) \qquad (2)$$

Where α and hν are the absorption coefficient and the photon energy, respectively, and A is the proportionality parameter. The Eg values of WO_3 and Zn-doped WO_3 structures were determined by plotting Tauc's plots using intercepts of the extrapolating the straight-line part plots between $(\alpha h\nu)^2$ versus photon energy (hυ) as exhibited in Figure 3b. As seen, the Eg values of WO_3 and Zn-doped WO_3 structures are determined to be ~3.12 and 2.83 eV, respectively. Because of the substitution of Zn^{2+} for W^{6+} and the formation of oxygen vacancies, the optical band gap of Zn-doped WO_3 decreases toward WO_3, increasing the electron carrier density as well as the electrical conductivity, resulting in fast charge transfer and the enhancement of photocatalytic activity of Zn-doped WO_3 structure under visible light irradiation [24, 58, 59].

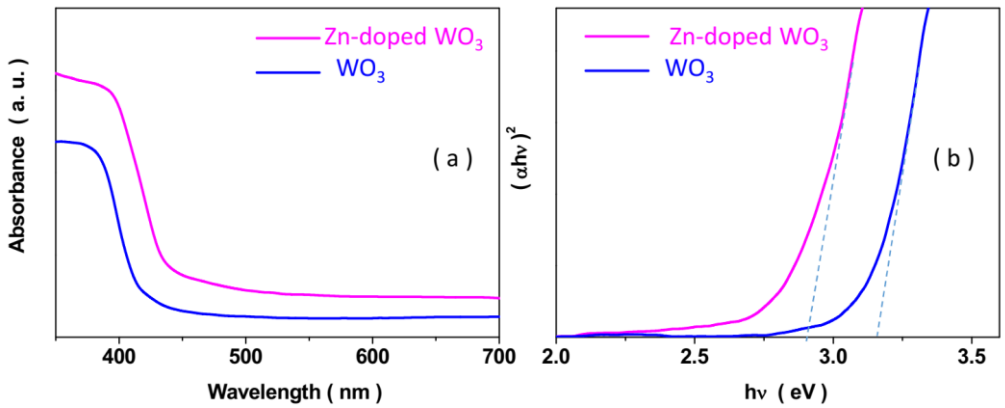

Figure 3. (a) UV–vis absorption spectra of the WO_3 and Zn-doped WO_3 and (b) Tauc's plots.

3.3. Electrochemical properties of photocatalysts

Figure 4 shows the EIS Nyquist and bode plots of WO_3 and Zn-doped WO_3 after exposure to visible light. The Nyquist plots show one semicircle, whose radius is related to the rate of electrochemical reaction at the electrode's surface, and a lower arc radius implies simpler electron transit and higher separation efficiency of photo-exited electrons and holes, as shown in Figure 4a. As can be seen, the arc radius of Zn-doped WO_3 is less than that of undoped WO_3, showing that the addition of Zn^{2+} improves photo-exited electron and hole separation and facilitates charge transfer [60-62], which is in agreement with the optical results. As a result, it enhances photo-electrochemical performance. The EIS data were analyzed with an equivalent electrical circuit model, as shown in Figure 4a, where R_s and R_{ct} represent solution resistance and charge transfer resistance, respectively, and CPE represents double layer capacitance [63, 64]. The parameters obtained from the equivalent circuit are summarized in Table 1, which implies the lower charge transfer resistance of Zn-doped WO_3. Furthermore, the lifetime (τ) of the photo-generated electrons can be estimated using the maximum peak frequency (f_{max}) in bode plots using the below equation [65, 66]:

$$\tau = \frac{1}{2\pi f_{max}} \qquad (3)$$

As observed from Table 1, The corresponding lifetime of photo-generated electrons in Zn-doped WO_3 is longer than that WO_3, which indicated to its largest separation efficiency and faster diffusion rate in Zn-doped WO_3 [67].

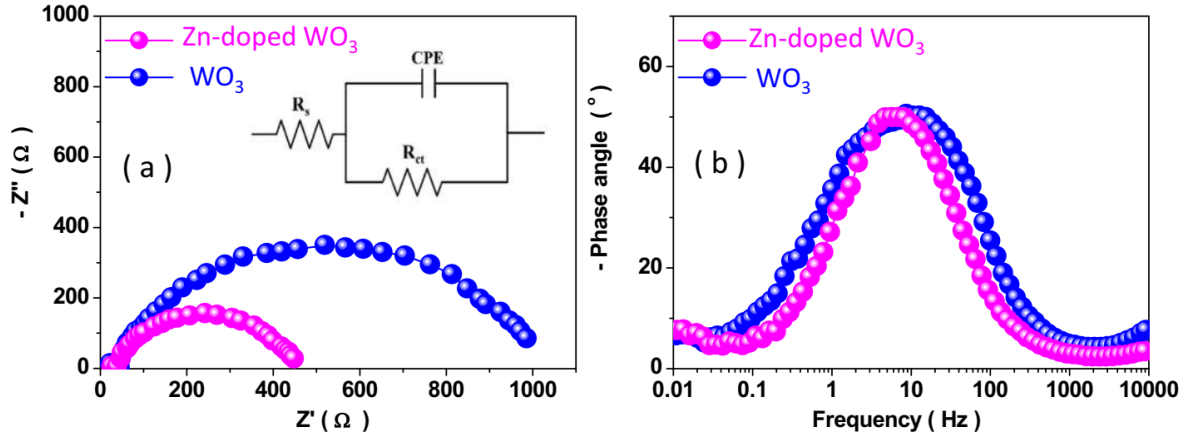

Figure 4. (a) The Nyquist and the equivalent circuit, and (b) bode plots for WO_3 and Zn-doped WO_3 upon visible light irradiation.

Table 1. The parameters obtained from the equivalent circuit.

Parameters	WO_3	Zn-doped WO_3
R_s (Ω)	36.65	34.69
R_{ct} (Ω)	981.1	420.2
τ (ms)	13.41	34.95

3.4. Photodegradation tests

Figure 5 shows the photocatalytic degradation efficiency of WO_3 and Zn-doped WO_3 for the treatment of 150 ml of 10 mg/L RhB solution when exposed to visible light. After 60 minutes of visible light irradiation, the degradation efficiency for the blank sample reaches 0.75 percent. After 5 minutes of visible light irradiation, the photocatalytic degradation efficiency of WO_3 and Zn-doped WO_3 is 24 percent and 43 percent, respectively. In current WO_3 and Zn-doped WO_3, the entire degradation efficiency is attained after 30 and 15 minutes of visible light irradiation, respectively. These findings support the high photocatalytic activity of Zn-doped WO3 under visible light irradiation, which is linked to three factors in good agreement with XRD, EIS, and optical analyses, including more efficient photo-generated electron-hole separation and quick charge transfer of Zn-doped WO_3 than WO_3, and a narrow band gap of the Zn-doped WO_3 that could explain the improved photocatalytic degradation of RhB under visible light irradiation. The photocatalytic mechanism of Zn-doped WO_3 catalyst is described as follows [68, 69]: the doping of Zn ions narrows the band gap of WO_3, because of the introduction of acceptor energy levels below the conduction level of WO_3 which makes it more photosensitizer to visible light, and under visible light irradiation, the Zn-doped WO_3 photocatalyst improves generation electron–hole pair and transfers a photogenerated electron from its valence band to the conduction band [70-72]. This leads to enhanced photodegradation performance.

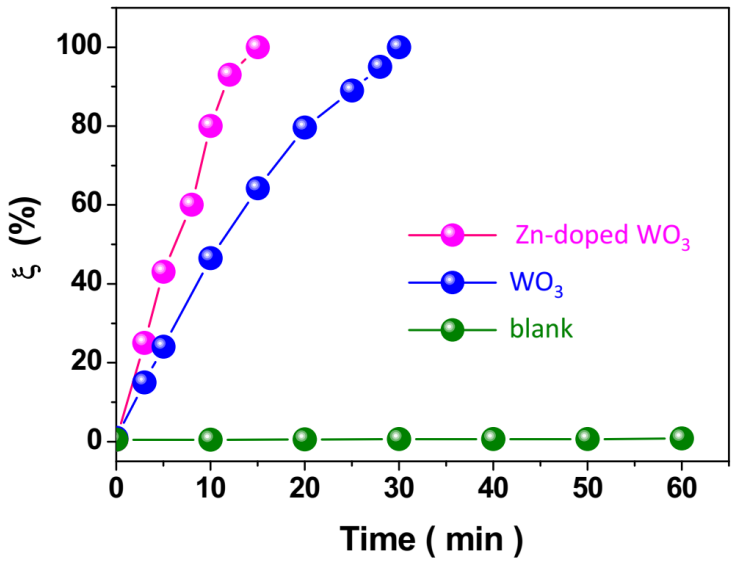

Figure 5. Degradation efficiency of blank sample (without photcatalyst), and photocatalytic degradation efficiency of WO_3 and Zn-doped WO_3 for the treatment of 150 ml of 10 mg/L RhB solution upon visible light irradiation

Figure 6 shows the effect of initial RhB concentrations (5, 10, 20, 50, and 100 mg/L) on the photocatalytic degradation efficiency of Zn-doped WO_3. As shown, the photocatalytic degradation

efficacy decreases as the concentration of RhB solution increases. After 10, 15, 25, 35, and 50 minutes of visible light irradiation, 100 percent treatment of 5, 10, 20, 50, and 100 mg/L of RhB occurs. Table 2 compares our findings to the photodegradation performance of various reported photocatalysts for the treatment of RhB. As found, Zn-doped WO_3 presents a high photocatalytic degradation efficiency due to the substitution of Zn^{2+} for W^{6+} and the creation of oxygen vacancies, which facilitate charge transfer and cause efficient separation of electron–hole pairs, as well as an increase in the photocatalytic activity of the Zn-doped WO_3 structure when exposed to visible light. Taking into account that Zn^{2+} ions form acceptor type centers in the crystal lattice of WO_3 make an improvement in the photoelectrochemical properties of Zn-doped WO_3 with respect to the undoped one [73, 74]. Cheng et al.[73] suggested that the commonality in all cation-doping Zn^{2+} ions rests with the formation of oxygen vacancies and the advent of color centers that absorb the visible light irradiation under the conditions of lowly doping. The fast degradation RhB solution can be considered as the novelty of this research between the reported ZnO and TiO_2 photocatalysts reported in Table 2. It can be related to the main drawback of ZnO and TiO_2 as photocatalysts, which is that the absorption wavelength of material lies in the UV region [28, 30]. This causes excessive electron–hole recombination. Additionally, ZnO has the ability to promote photochemical corrosion [75]. Modifications to ZnO and TiO_2 such as thermal treatment and/or doping the materials with other metal ions could enhance photocatalytic activity through limiting the recombination of electron–hole pairs and improving the absorption of UV light [31, 32]. In this research, Zn-doped WO_3 presents the fast degradation RhB solution solution upon visible light irradiation to enhance the cost effectiveness of the catalytic process.

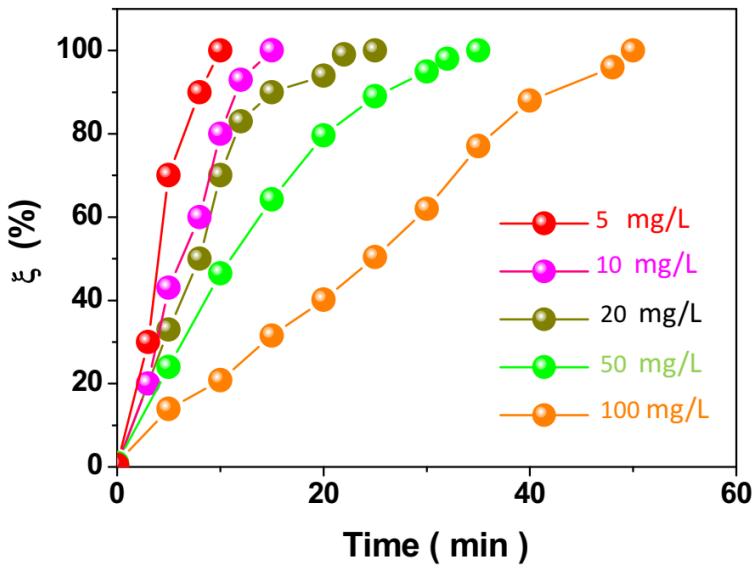

Figure 6. The influence of initial RhB concentrations (5, 10, 20, 50 and 100 mg/L) on the photocatalytic degradation efficiency of Zn-doped WO_3.

Table 2. Photodegradation performance of Zn-doped WO_3 and various reported photocatalysts for the treatment of RhB.

Photocatalyst	**Amount of RhB (mg/L)**	**Light source**	**Degradation efficiency (%)**	**Degradation time (minute)**	**Ref.**
TiO_2-P25/Cu^{2+}	8.2	UV	100	60	[31]
ZnO	10	UV	95	70	[30]
$Pb_3Nb_4O_{13}$	10	Visible	100	125	[29]
TiO_2-P25	16.94	UV	80	180	[28]
$NaBiO_3$	20	Visible	100	30	[27]
Ag/ZnO-TiO_2	50	UV	83.2	30	[32]
Zn-doped WO_3	5	Visible	100	10	This work
	10			15	
	20			25	
	50			35	
	100			50	

3.5. Treatment of real textile effluent

The practical photocatalytic degradation capability of Zn-doped WO_3 was investigated for the treatment of 150 mL of 5 mg/L RhB solution collected from a textile mill (Shanghai, China) and compared to the sample prepared with deionized wastewater (RhB2). Figure 7 shows the photodegradation efficiency of RhB1 and RhB2 after exposure to visible light for 25 and 10 minutes, respectively. Because of the presence of additional pollutants in textile wastewater, thorough treatment of RhB1 generated from real textile effluent takes longer. The results demonstrate the efficient photodegradation of Zn-doped WO_3 for the treatment of RhB in genuine textile effluent.

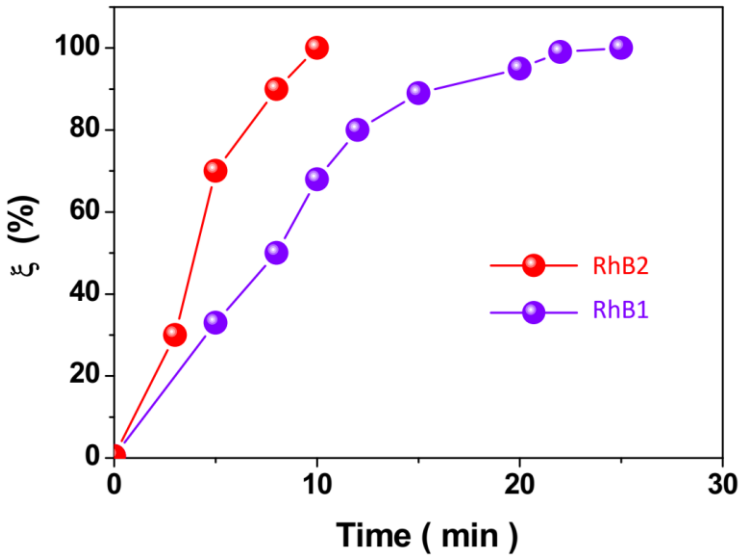

Figure 7. The photocatalytic degradation efficacy of 150 mL of 5 mg/L RhB solution made from real textile effluent (RhB1) and sample prepared with deionized wastewater (RhB2) using Zn-doped WO_3 upon visible light irradiation.

4. CONCLUSION

The practical photocatalytic degradation capability of Zn-doped WO_3 was investigated for the treatment of 150 mL of 5 mg/L RhB solution collected from a textile mill (Shanghai, China) and compared to the sample prepared with deionized wastewater (RhB2). Figure 7 shows the photodegradation efficiency of RhB1 and RhB2 after exposure to visible light for 25 and 10 minutes, respectively. Because of the presence of additional pollutants in textile wastewater, thorough treatment of RhB1 generated from real textile effluent takes longer. The results demonstrate the efficient photodegradation of Zn-doped WO_3 for the treatment of RhB in genuine textile effluent. According to electrochemical experiments, the lifespan of photo-generated electrons in Zn-doped WO_3 was longer than that of WO_3, indicating that Zn-doped WO_3 had the highest separation efficiency and the fastest diffusion rate. The entire degradation efficiency of 150 mL of 10 mg/L RhB solution was reached after 30 and 15 minutes of visible light irradiation in current WO_3 and Zn-doped WO_3, respectively, according to the photodegradation assays. The photocatalytic degradation capability of Zn-doped WO_3 was tested for the treatment of 150 mL of 5 mg/L RhB solution prepared from real textile effluent, and the results confirmed that Zn-doped WO_3 has a high photocatalytic activity when exposed to visible light for the treatment of RhB from real textile effluent.

References

1. J. Wess and D. Archer, *Food and Chemical Toxicology*, 20 (1982) 9.
2. T. Zhang, X. Wu, S.M. Shaheen, H. Abdelrahman, E.F. Ali, N.S. Bolan, Y.S. Ok, G. Li, D.C. Tsang and J. Rinklebe, *Journal of hazardous materials*, 425 (2022) 127906.
3. C. Yu, X. Chen, N. Li, Y. Zhang, S. Li, J. Chen, L. Yao, K. Lin, Y. Lai and X. Deng, *Environmental Science and Pollution Research*, 29 (2022) 18423.
4. X. Cui, C. Li, Y. Zhang, Z. Said, S. Debnath, S. Sharma, H.M. Ali, M. Yang, T. Gao and R. Li, *Journal of Manufacturing Processes*, 80 (2022) 273.
5. K.-H. Wang, Y.-M. Wang, L.-H. Chiu, T.-C. Chen, Y.-H. Tsai, C.S. Zuo, K.-C. Chen, C.A. Changou and W.-F.T. Lai, *PloS one*, 13 (2018) e0192047.
6. Y. Yang, H. Zhu, X. Xu, L. Bao, Y. Wang, H. Lin and C. Zheng, *Microporous and Mesoporous Materials*, 324 (2021) 111289.
7. B. Li, C. Li, Y. Zhang, Y. Wang, D. Jia and M. Yang, *Chinese Journal of Aeronautics*, 29 (2016) 1084.
8. J. Riordon, D. Sovilj, S. Sanner, D. Sinton and E.W. Young, *Trends in biotechnology*, 37 (2019) 310.
9. Z. Wu, C. Li, F. Zhang, S. Huang, F. Wang, X. Wang and H. Jiao, *Journal of Materials Chemistry C*, 10 (2022) 7443.
10. M. Khosravi, *Open Access Macedonian Journal of Medical Sciences*, 8 (2020) 553.
11. H. Li, Y. Zhang, C. Li, Z. Zhou, X. Nie, Y. Chen, H. Cao, B. Liu, N. Zhang and Z. Said, *Korean Journal of Chemical Engineering*, 39 (2022) 1107.
12. Y. YANG, M. YANG, C. Li, R. Li, Z. Said, H.M. Ali and S. SHARMA, *Frontiers of Mechanical Engineering*, (2022) 1.
13. H. Liu, J. Yang, Y. Jia, Z. Wang, M. Jiang, K. Shen, H. Zhao, Y. Guo, Y. Guo and L. Wang, *Environmental Science & Technology*, 55 (2021) 10734.

14. D. Jia, Y. Zhang, C. Li, M. Yang, T. Gao, Z. Said and S. Sharma, *Tribology International*, 169 (2022) 107461.
15. J. Rouhi, H.K. Malayeri, S. Kakooei, R. Karimzadeh, S. Alrokayan, H. Khan and M.R. Mahmood, *International Journal of Electrochemical Science*, 13 (2018) 9742.
16. A.A. Al-Gheethi, Q.M. Azhar, P.S. Kumar, A.A. Yusuf, A.K. Al-Buriahi, R.M.S.R. Mohamed and M.M. Al-Shaibani, *Chemosphere*, 287 (2022) 132080.
17. T. Li, D. Shang, S. Gao, B. Wang, H. Kong, G. Yang, W. Shu, P. Xu and G. Wei, *Biosensors*, 12 (2022) 314.
18. D.R. Sulistina and S. Martini, *Journal of Public Health Research*, 9 (2020) 1.
19. H. Li, Y. Zhang, C. Li, Z. Zhou, X. Nie, Y. Chen, H. Cao, B. Liu, N. Zhang and Z. Said, *The International Journal of Advanced Manufacturing Technology*, 120 (2022) 1.
20. H. Maleh, M. Alizadeh, F. Karimi, M. Baghayeri, L. Fu, J. Rouhi, C. Karaman, O. Karaman and R. Boukherroub, *Chemosphere*, (2021) 132928.
21. M. Isanejad, M. Arzani, H.R. Mahdavi and T. Mohammadi, *Journal of Molecular Liquids*, 225 (2017) 800.
22. R. Shokoohi, M. Salari, R. Safari, H. Zolghadr Nasab and S. Shanehsaz, *International Journal of Environmental Analytical Chemistry*, 101 (2021) 2629.
23. L. Feng, X.H. Li, W.C. Lu, Z. Liu, C. Xu, Y. Chen, H.L. Zheng. International Journal of Biological Macromolecules, 150 (2020) 617.
24. R. Savari, J. Rouhi, O. Fakhar, S. Kakooei, D. Pourzadeh, O. Jahanbakhsh and S. Shojaei, *Ceramics International*, 47 (2021) 31927.
25. S.-H. Chang, K.-S. Wang, H.-C. Li, M.-Y. Wey and J.-D. Chou, *Journal of Hazardous Materials*, 172 (2009) 1131.
26. L. Feng, J.J. Liu, Z.C. Guo, T.Y. Pan, J.H. Wu, X.H. Li, B.Z. Liu and H.L. Zheng, Separation and Purification Technology, 285 (2021)120314.
27. K. Yu, S. Yang, H. He, C. Sun, C. Gu and Y. Ju, *The Journal of Physical Chemistry A*, 113 (2009) 10024.
28. E.T. Soares, M.A. Lansarin and C.C. Moro, *Brazilian Journal of Chemical Engineering*, 24 (2007) 29.
29. O. Merka, V. Yarovyi, D.W. Bahnemann and M. Wark, *The Journal of Physical Chemistry C*, 115 (2011) 8014.
30. Q.I. Rahman, M. Ahmad, S.K. Misra and M. Lohani, *Materials Letters*, 91 (2013) 170.
31. N. Barka, S. Qourzal, A. Assabbane, A. Nounah and Y. Ait-Ichou, *Journal of Photochemistry and Photobiology A: Chemistry*, 195 (2008) 346.
32. L. Li, X. Zhang, W. Zhang, L. Wang, X. Chen and Y. Gao, *Colloids and Surfaces A: Physicochemical and Engineering Aspects*, 457 (2014) 134.
33. X. Chen, L. Li, Y. Shan, D. Zhou, W. Cui and Y. Zhao, *Journal of Energy Chemistry*, 70 (2022) 502.
34. T. Gao, Y. Zhang, C. Li, Y. Wang, Q. An, B. Liu, Z. Said and S. Sharma, *Scientific reports*, 11 (2021) 1.
35. M. Khosravi, *European journal of translational myology*, 31 (2021) 9411.
36. K. Santhi, C. Rani, R. Dhilip Kumar and S. Karuppuchamy, *Journal of Materials Science: Materials in Electronics*, 26 (2015) 10068.
37. J.M. Quintana-Melgoza, A. Gómez-cortés and M. Avalos-Borja, *Reaction Kinetics and Catalysis Letters*, 76 (2002) 131.
38. Y. Shan, L. Li, X. Chen, S. Fan, H. Yang and Y. Jiang, *ACS Energy Letters*, 7 (2022) 2289.
39. X. Wu, C. Li, Z. Zhou, X. Nie, Y. Chen, Y. Zhang, H. Cao, B. Liu, N. Zhang and Z. Said, *The International Journal of Advanced Manufacturing Technology*, 117 (2021) 2565.
40. M.I. Osotsi, D.K. Macharia, B. Zhu, Z. Wang, X. Shen, Z. Liu, L. Zhang and Z. Chen, *Progress in Natural Science: Materials International*, 28 (2018) 408.

41. W. Liu, J. Li, J. Zheng, Y. Song, Z. Shi, Z. Lin and L. Chai, *Environmental Science & Technology*, 54 (2020) 11971.
42. X. Wang, C. Li, Y. Zhang, H.M. Ali, S. Sharma, R. Li, M. Yang, Z. Said and X. Liu, *Tribology International*, 174 (2022) 107766.
43. Y. Cui, L. Pan, Y. Chen, N. Afzal, S. Ullah, D. Liu, L. Wang, X. Zhang and J.-J. Zou, *RSC advances*, 9 (2019) 5492.
44. M. Liu, C. Li, Y. Zhang, Q. An, M. Yang, T. Gao, C. Mao, B. Liu, H. Cao and X. Xu, *Frontiers of Mechanical Engineering*, 16 (2021) 649.
45. M. Khosravi, *Pharmacopsychiatry*, 55 (2022) 16.
46. D. Madhan, M. Parthibavarman, P. Rajkumar and M. Sangeetha, *Journal of Materials Science: Materials in Electronics*, 26 (2015) 6823.
47. V. Hariharan, V. Aroulmoji, K. Prabakaran, B. Gnanavel, M. Parthibavarman, R. Sathyapriya and M. Kanagaraj, *Journal of Alloys and Compounds*, 689 (2016) 41.
48. D. Ge, H. Yuan, J. Xiao and N. Zhu, *Science of The Total Environment*, 679 (2019) 298.
49. H. Karimi-Maleh, H. Beitollahi, P.S. Kumar, S. Tajik, P.M. Jahani, F. Karimi, C. Karaman, Y. Vasseghian, M. Baghayeri and J. Rouhi, *Food and Chemical Toxicology*, (2022) 112961.
50. K. Salehi, A. Kordlu and R. Rezapour-Nasrabad, *Studies on Ethno-Medicine*, 14 (2020) 24.
51. S.S. Kalanur, *Catalysts*, 9 (2019) 456.
52. R. Hassanzadeh, A. Siabi-Garjan, H. Savaloni and R. Savari, *Materials Research Express*, 6 (2019) 106429.
53. X. Cui, C. Li, Y. Zhang, W. Ding, Q. An, B. Liu, H.N. Li, Z. Said, S. Sharma, R. Li and S. Debnath, *Frontiers of Mechanical Engineering*, (2022) 1.
54. X. Li, M. Ai, X. Zhang, J.-J. Zou and L. Pan, *International Journal of Hydrogen Energy*, 47 (2022) 13641.
55. Q. Guan, G. Zeng, J. Song, C. Liu, Z. Wang and S. Wu, *Journal of environmental management*, 293 (2021) 112961.
56. Z. Wang, A. He and L. Liu, *International Journal of Electrochemical Science*, 17 (2022) 220645.
57. L. Tang, Y. Zhang, C. Li, Z. Zhou, X. Nie, Y. Chen, H. Cao, B. Liu, N. Zhang and Z. Said, *Chinese Journal of Mechanical Engineering*, 35 (2022) 1.
58. K. Paipitak, W. Techitdheera, S. Porntheeraphat and W. Pecharapa, *Energy Procedia*, 34 (2013) 689.
59. H. Savaloni and R. Savari, *Materials Chemistry and Physics*, 214 (2018) 402.
60. Y.-H. Xiao, C.-Q. Xu and W.-D. Zhang, *Journal of Solid State Electrochemistry*, 21 (2017) 3355.
61. Y. Wang, X. Wu, J. Liu, Z. Zhai, Z. Yang, J. Xia, S. Deng, X. Qu, H. Zhang and D. Wu, *Journal of Environmental Chemical Engineering*, 10 (2022) 107091.
62. R. Rezapour-Nasrabad, *Archivos Venezolanos de Farmacología y Terapéutica*, 40 (2021) 455.
63. F. Bentiss, M. Outirite, M. Traisnel, H. Vezin, M. Lagrenée, B. Hammouti, S. Al-Deyab and C. Jama, *International Journal of Electrochemical Science*, 7 (2012) 1699.
64. H. Karimi-Maleh, C. Karaman, O. Karaman, F. Karimi, Y. Vasseghian, L. Fu, M. Baghayeri, J. Rouhi, P. Senthil Kumar and P.-L. Show, *Journal of Nanostructure in Chemistry*, (2022) 1.
65. J. Sun, H. Guo, L. Zhao, S. Wang, J. Hu and B. Dong, *International Journal of Electrochemical Science*, 12 (2017) 7941.
66. W. Zhang, S. Chang, J. Gu, S. Yao and H. Wang, *International Journal of Electrochemical Science*, 14 (2019) 7166.
67. C. Du, D. Li, Q. He, J. Liu, W. Li, G. He and Y. Wang, *Physical Chemistry Chemical Physics*, 18 (2016) 26530.
68. Y. Wang, C. Li, Y. Zhang, M. Yang, B. Li, L. Dong and J. Wang, *International Journal of Precision Engineering and Manufacturing-Green Technology*, 5 (2018) 327.

69. J. Zhang, C. Li, Y. Zhang, M. Yang, D. Jia, G. Liu, Y. Hou, R. Li, N. Zhang and Q. Wu, *Journal of cleaner production*, 193 (2018) 236.
70. P. Sivakarthik, V. Thangaraj and M. Parthibavarman, *Journal of Materials Science: Materials in Electronics*, 28 (2017) 5990.
71. L. Dai, Z. Wang, T. Guo, L. Hu, Y. Chen, C. Chen, G. Yu, L.Q. Ma and J. Chen, *Chemosphere*, 293 (2022) 133576.
72. H. Karimi-Maleh, R. Darabi, M. Shabani-Nooshabadi, M. Baghayeri, F. Karimi, J. Rouhi, M. Alizadeh, O. Karaman, Y. Vasseghian and C. Karaman, *Food and Chemical Toxicology*, 162 (2022) 112907.
73. X. Cheng, W. Leng, D. Liu, J. Zhang and C. Cao, *Chemosphere*, 68 (2007) 1976.
74. M. Arshad, S. Ehtisham-ul-Haque, M. Bilal, N. Ahmad, A. Ahmad, M. Abbas, J. Nisar, M. Khan, A. Nazir and A. Ghaffar, *Materials Research Express*, 7 (2020) 015407.
75. L. Zhang, M. Jeem, K. Okamoto and S. Watanabe, *Scientific reports*, 8 (2018) 1.

© 2022 The Authors. Published by ESG (www.electrochemsci.org). This article is an open access article distributed under the terms and conditions of the Creative Commons Attribution license (http://creativecommons.org/licenses/by/4.0/).